563564

Differences in the microstructure were observed by light microscopy in alloys grown at rates ranging from 7.6 to 508 mm/hr. But, compression testing ...

Effect of Microstructure on Creep in Directionally Solidified NiAl-31Cr-3Mo

J.Daniel Whittenberger[1], S.V. Raj[1] and I.E. Locci[2]

[1] NASA-Glenn Research Center, Cleveland, OH, USA 44135
[2] Case Western Reserve University at GRC, Cleveland, OH, USA 44135

Abstract

The 1200 to 1400 K slow strain rate characteristics of the directionally solidified (DS) eutectic Ni-33Al-31Cr-3 Mo have been determined as a function of growth rate. While differences in the light optical level microstructure were observed in alloys grown at rates ranging from 7.6 to 508 mm/h, compression testing indicated that all had essentially the same strength. The exception was Ni-33Al-31Cr-3Mo DS at 25.4 mm/h which was slightly stronger than the other growth velocities; no microstructual reason could be found for this improvement. Comparison of the ~1300 K properties revealed that four different DS NiAl-34(Cr,Mo) alloys have a similar creep resistance which suggests that there is a common, but yet unknown, strengthening mechanism.

Introduction

Directionally solidified (DS) systems based on the NiAl-34(at. %)Cr eutectic are under consideration as possible replacements for Ni-based superalloys exposed to severe temperature, stress, and environment conditions. The unique microstructures created during directional solidification, in the form of aligned ~1 μm diameter Cr fibers in a NiAl matrix for NiAl-34Cr [1] or aligned micron thick alternating NiAl and α-(Cr,Mo) lamella in NiAl-(34-x)-xMo (x >0.6%) [2], result in both good elevated temperature creep strength and reasonable room temperature toughness [3-9]. In particular the improvement in creep properties is remarkable compared to those of the constituents: for example the 1300 K - 10^{-7} s^{-1} strength of DS NiAl-34Cr is about 100 MPa [3]; whereas polycrystalline NiAl [10], [100]-oriented NiAl single crystals [3,11] and large grain size Cr [12,13] would require only 10 to15 MPa to deform at these conditions.

Since the early work by Cline and Walter [2] did not report a clear dependency between the "goodness" of alignment and mechanical properties for NiAl-34Cr based eutectics, NiAl-31Cr-3Mo was DS at rates ranging from 12.7 to 508 mm/h and subjected to both room temperature toughness and elevated temperature slow strain rate compressive testing [6]. The initial results indicated that 1200 and 1300 K strength properties were similar for all the growth

degree of quality > OPTIONS

rates. This paper extends the preliminary study on the elevated temperature properties of DS NiAl-31Cr-3Mo as a function of growth rate to include an as-cast alloy, a very slowly grown eutectic (7.6 mm/h), testing at 1400 K, and a few constant load creep experiments to achieve slower strain rates. The strength properties of DS NiAl-31Cr-3Mo are examined in light of the available microstuctural data and are compared to those for other NiAl-34Cr based eutectics. Lastly, potential mechanisms responsible for the high strength of DS NiAl-(Cr,Mo) eutectics are examined.

Experimental Procedures

The methods used to produced aligned eutectic bars at directional solidification growth rates ranging from 7.6 to 508 mm/h are completely discussed in [6,7,14]. Since the original bar grown at 7.6 mm/h in [6] was significantly off chemistry (28.6Al instead of 33Al), a new bar was DS'd at this rate utilizing an as-cast rod with the correct composition. Compression specimens were taken from the aligned region of each DS'd bar by wire electrodischarge machining (EDM). The compression specimens were 8 x 4 x 4 mm in size with the 8 mm sample length parallel to the growth axis, and they were tested in the as-EDM'ed surface condition. A set of compression samples was also machined from an as-cast rod (the one partially utilized for the DS run at 12.7 mm/h) in order to access the strength improvement from directional solidification; the long axis of these samples was parallel to the length of the casting.

Elevated temperature compressive strength properties were mainly determined by constant velocity testing which was supplemented with a few constant load creep tests. A screw driven universal testing machine was utilized for constant velocity testing, where samples were compressed between two solid push bars at 1200, 1300 and 1400 K in air at crosshead rates that varied from 1.7×10^{-2} to 1.6×10^{-6} mm/s. The autographically recorded load - time curves were converted to true stresses, strains and strain rates via the offset method in combination with a normalization to the final specimen length and the assumption of a constant volume. Constant load compressive creep experiments were undertaken in a lever arm creep machine, where time dependent deformation was determined by measurement of the relative positions of the ceramic push bars applying the load to the specimen. All the contraction - time data from creep testing were normalized with respect to the final specimen length and converted into true stresses and strains assuming that the sample volume was constant.

Results

Materials -- Characterization of the chemistry of the individual as-cast rods and DS bars are reported in [6,7,14], and the compositional control was very good. Grouping all the bars DS between 7.6 and 508 mm/h together, the average composition was Ni-33.4Al-31.2Cr-2.9Mo with standard deviations of 0.6 at % for Al & Cr, and 0.1 % for Mo; each bar also contained about 0.14 % Si and small amounts of C (~0.06%), N (~0.001%) and O (~0.02%). The as-cast rod, which was compression tested in this study, had the following composition: Ni-33.3Al-31.1Cr-3.0Mo with 0.013Si-0.07C-0.007N and 0.07O. The higher Si content in the DS rods in comparison to the as-cast bars is probably the result of long exposures during solidification in crucibles which contained a SiO_2 binder.

Transverse microstructural sections of the DS'd rods illustrated that large diameter lamellar eutectic grains with sharp boundaries formed (Fig. 1(a)) at and below growth rates of 12.7 mm/h, while at higher velocities ~200 μm diameter cellular structures bounded by relatively thick intercellular regions developed (Fig. 1(b)). The lamellar eutectic grains were composed of

alternating NiAl and α-(Cr,Mo) plates while the cells contained lamellae in a radial-like pattern which some cases terminated and in other cases coarsened to form the intercellular regions. The as-cast microstructure transverse to the casting direction is illustrated in Fig. 1(c), where cells containing a fine pearlitic structure were surrounded by relatively wide intercellular regions. Examination of longitudinal sections of the DS rods [6,14] indicated that both the lamellar eutectic grains and cellular grains were mm's in length; however the lamellae were not always parallel to the growth direction. Additional details about the microstructures of DS NiAl-31Cr-3Mo as a function of growth rate are given in [6] and extensive quantitative measurements are presented in [14].

Compressive Properties --Examples of the true compressive stress - strain diagrams from 1300 K constant velocity testing and constant load compressive creep curves are presented in Fig. 2. The stress - strain curves for both the as-cast alloy (Fig. 2(a)) and a DS alloy (Fig. 2(b)) demonstrate rapid work hardening through ~1 % strain followed by continued deformation at a more or less constant flow stress or slow strain softening after reaching a maximum stress. Testing of all the directionally solidified bars of Ni-33Al-31Cr-3Mo between 1200 and 1400 K and the as-cast alloy at 1200 and 1400 K produced stress - strain curves similar to those shown in Figs. 2 (a,b). Creep testing of the directionally solidified alloys (Fig. 2(c)) produced normal behavior where primary creep was followed by steady state creep. Several DS samples were step loaded to higher stress levels which did not lead to a normal primary creep response, i.e., additional hardening. ~~Invariably~~ after a load increase, these samples transitioned immediately into steady state creep which eventually lead to tertiary creep.

Instead,

True flow stress (σ) - strain rate ($\dot{\varepsilon}$) behavior for the as-cast Ni-33Al-31Cr-3Mo (solid circles) and all the directionally solidified bars is presented in Fig. 3 as a function of temperature (T). In these plots the flow stresses taken from constant velocity testing are represented by the stress at 1 % strain from the stress - strain curves (Figs. 2(a,b)), while the flow stresses from creep testing are arithmetic averages calculated over the steady state regimes (Fig. 2(c)). By visual inspection directional solidification provides a clear strength advantage over simple casting; furthermore the elevated temperature strength properties of DS Ni-33Al-31Cr-3Mo do not appear to be strongly dependent on growth rate.

Examples of the temperature dependence of the true flow stress - strain rate results are illustrated in Fig. 4. Where appropriate, the σ-$\dot{\varepsilon}$-T data for all the alloys were fitted by linear regression techniques to a temperature-compensated power law,

$$\dot{\varepsilon} = A\,\sigma^{n}\exp(-Q/(RT)), \qquad (1)$$

where A is a constant, n is the stress exponent, Q is the activation energy for deformation and R is the universal gas constant. The values for A, n, Q and the standard deviations for the stress

exponent (δ_n) and activation energy (δ_Q) as well as the coefficient of determination (R_d^2) for each fit are given in Table 1, and the curves in Fig. 4 are the result of such fits. While eqn (1) can describe the data for each material condition, examination of the fit parameters for Ni-33Al-31Cr-3Mo DS at rates from 7.6 to 508 mm/h show a wide range in values even though all seven alloys possess similar strengths at each test temperature (Fig. 3). Because of the similarity of strength among the versions of Ni-33Al-31Cr-3Mo, this large range in descriptive parameters is probably an artifact of the least squares approach.

Table 1. Temperature Compensated Power Law Parameters for As-Cast and Directional Solidified Ni-33Al-31Cr-3Mo.

Growth Velocity, mm/h	A, s^{-1}	n	δ_n	Q, kJ/mol	δ_Q,	R_d^2	Data points not utilized in the analyses
7.6	1.29×10^4	6.37	0.38	-588.2	38.0	0.977	1200 K > 10^{-5} s^{-1} & 1300 K - 10^{-3} s^{-1}
12.7	9.21	4.43	0.20	-405.1	29.9	0.989	1200 K > 10^{-5} s^{-1}, 1300 K > 10^{-4} s^{-1} & 1400 K - 10^{-3} s^{-1}
As Cast (12.7)	0.714	4.83	0.33	-374.7	31.8	0.971	1200 K - 10^{-4} s^{-1} & 1300 K - 10^{-3} s^{-1}
25.4	3.05×10^3	5.61	0.18	-539.4	24.3	0.991	1200 K > 10^{-5} s^{-1} & 1300 K - 10^{-3} s^{-1}
50.8	5.96×10^1	4.88	0.16	-450.0	22.4	0.989	1200 K > 10^{-5} s^{-1} & 1300 K - 10^{-4} s^{-1}
127	1.47×10^1	4.53	0.35	-475.0	35.2	0.975	1200 K > 10^{-5} s^{-1}
254	2.20×10^3	5.58	0.42	-531.2	39.9	0.965	1200 K > 10^{-5} s^{-1} & 1300 K - 10^{-3} s^{-1}
508	4.27	5.58	0.41	-460.1	34.7	0.969	1200 K - 10^{-4} s^{-1} & 1300 K - 10^{-3} s^{-1}

To determine if any one directional solidification growth rate had a strength advantage, the individual sets of data were tested against each other employing a dummy variable in a multiple linear regression analyses. The results from these statistical analyses are shown in Fig. 5. Six of the seven DS rates {7.6,12.7, 50.8,127, 254 and 508 mm/h, open symbols in Fig. (6)} possessed 1200-1400 K compressive properties which could not be separated from one another, where

$$\dot{\varepsilon} = 1000\, \sigma^{4.99} \exp(-487.3/(RT)), \qquad (2)$$

The solid curves in Fig. 5 illustrate the fit of eqn (2), and they can be compared to the behavior of Ni-33Al-31Cr-3Mo DS at 25.4 mm/h (solid symbols) which demonstrates a small strength advantage over the other six growth conditions. While the behavior of the 25.4 mm/h alloy is accurately characterized by n = 5.61 and Q = -539.4 kJ/mol (R_d^2 = 0.991, Table 1), use of a dummy variable can force a fit to have the same stress exponent and activation energy as eqn (2). Thus the behavior of Ni-33Al-31Cr-3Mo DS at 25.4 mm/h can be reflected by a lower pre-exponent term, where

$$\dot{\varepsilon} = 519\, \sigma^{4.99} \exp(-487.3/(RT)) \qquad (3)$$

which corresponds to an ~14 % strength advantage, as illustrated by the dashed lines in Fig. 5. Taken together eqns (2,3) are able to describe the temperature compensated power law characteristics of Ni-33Al-31Cr-3Mo directionally solidified over a 60 fold range in growth rates with a R_d^2 of 0.947 and δ_n = 0.14 and δ_Q = 18.1 kJ/mol.

Discussion

Over the current range in testing (Figs. 3,5) the 1200 - 1400 K strength of Ni-33Al-31Cr-3Mo DS at 25.4 mm/h is statistically slightly better than that observed for slower or faster growth rates. Comparison of this improvement to the detailed microstructural measurements made on transverse sections by Raj and Locci [14] and the estimates of the minimum grain/cell length in

the longitudinal/DS growth direction (Fig. 6) do not reveal any obvious microstructural feature responsible for the increase. Neither the minimum grain/cell length, average cell diameter, intercellular region width (area fraction), interlamellar spacing nor NiAl lamella width for the alloy grown at 25.4 mm/h display any characteristic which separates it from other DS rates. Thus, the reason for the additional strength of the alloy grown at 25.4 mm/h is not known; most certainly, if there is further interest in this alloy system, more bars should be directionally solidified at this velocity and tested to confirm the current behavior.

With regard to the elevated temperature strength of NiAl-31Cr-3Mo, the 1200 - 1400 K compressive data in Fig. 4 indicate that directional solidification does produce a significant strength increase compared to simple casting. While these results, as well those for other NiAl-34Cr eutectics w/o Mo additions [3-9], demonstrate that directional solidification is effective, the mechanism(s) for improvement are not clear. Fig. 7 illustrates the compressive properties for several DS NiAl-(Cr,Mo) alloys at/near 1300 K, and, even though the individual stress exponents range from ~5.6 to 8.2, the overall behavior suggests that, to a good first approximation, NiAl-34Cr, NiAl-33Cr-1Mo, NiAl-31Cr-3Mo and NiAl-28Cr-6Mo all possess equivalent strengths Thus, while there are many significant differences among these DS eutectics [1,2], it appears that strengthening might have a common origin.

Kollura and Pollock [16] have recently applied numerical analysis to model creep of DS NiAl-34Cr at 1273 K, and they basically concluded that creep parallel to the Cr fiber axis takes place by plastic deformation of the NiAl matrix which transfer load to elastic Cr fibers. As partial support for this mechanism, they calculated much higher creep rates than those measured in this eutectic if it was assumed that the Cr-fibers crept at a rate one hundredth of that for the NiAl matrix. Additionally, they cited transmission electron microscope (TEM) evidence [17] that shows (1) the Cr fibers were dislocation-free and (2) no substantial differences in the NiAl substructure existed between deformed NiAl-34Cr and single phase NiAl.

Their latter contention is at odds with other observations of substructure in NiAl deformed at elevated temperature, where, for example, it was demonstrated that doping NiAl with 0.09N will produce a distribution of AlN particles which can anchor a small subgrain structure [18]. In fact the AlN particles forced the matrix to behave as a constant substructure material which was stronger than single phase NiAl [10,11] and essentially followed the behavior predicted by Sherby, et al.[19] with a high stress exponent ($n \approx 8$) and activation energy near that for volume diffusion. If subgrains do develop in NiAl during the elevated deformation of DS NiAl-(Cr,Mo) eutectics, then the NiAl/α-(Cr,Mo) interfaces should act as pinning points which would force the subgrains to be of the same dimension as the lamella thickness (~1 μm, Fig. 7) and lead to constant structure strengthening.

Since well developed subgrains have also been found in crept pure Cr [12], one could anticipate substructure strengthening via pining at Cr(Mo)/NiAl interfaces in the Cr fibers or α-(Cr,Mo) lamella. However, in view of Kolluru's observation of dislocation-free Cr fibers after 1273 K creep [17], this might not be the case. While the absence of dislocations was viewed to be evidence of elastic behavior [16], other interpretations of dislocation-free fibers in deformed eutectic are possible. For example if Cr offers very little resistance to dislocation motion within the fiber once the dislocation is through the interface, it could quickly glide across and leave. The resistance to glide should be equal to the Orowan stress σ_O which is approximately Gb/l, where G is the shear modulus, b is the magnitude of the burgers vector and l is the fiber diameter/lamella thickness. From the G,b values for Cr given by Frost and Ashby [20] at 1300 K, $\sigma_O = 24.3/l$ Pa•m which would range from about 8 MPa for a 3 micron diameter/spacing to 50 MPa for a 0.5 micron diameter/spacing. In view of the ~1.5 μm Cr-fiber diameter [3,4], the

lamella thickness (Fig. 6) and the 1300 K strength levels demonstrated for the DS NiAl-(Cr,Mo) eutectics in Fig. 7, the fibers/plates should not restrict glide.

The limitation of Cr-fibers to only elastic deformation during elevated temperature creep of DS NiAl-34Cr is also drawn into question by several other studies. Examination of 1200 - 1400 K compressive creep behavior of cryomilled NiAl containing about 10 vol % Cr [13] indicated that the strength of these composites followed the Rule-of-Mixtures, where Cr deformed at the rates described by Stephens and Klopp [12]. A similar observation was made by Venkatesh and Dunand [21], who studied the elevated temperature compressive properties of continuous, unidirectional W-wires imbedded in NiAl, and they found that the creep strength of composites containing from 5 to 20 vol % W could be described by the Rule-of-Mixtures. Lastly by analogy to W wire, one would expect substructure free Cr-fibers to be relatively weak and prone to deformation since recrystallization of worked W-wires has been shown to severely reduce their creep strength [21, 22].

Clearly, there is a need for detailed TEM studies of creep deformed directionally solidified NiAl-(Cr,Mo) eutectics to increase our understanding of deformation and strengthening in these materials. In reality, very little is known about dislocation structures in any of these alloys. To date the available information consists of the observation of an interfacial network of dislocations [3,5,23,24] to accommodate the semi-coherent interface between NiAl and α-(Cr,Mo) in as-grown eutectics and the citation of no unusual substructure in NiAl nor dislocations in Cr-fibers in crept NiAl-34Cr [16]. Any future effort to examine the behavior of DS NiAl-(Cr,Mo) at elevated temperature should include a commitment for a thorough TEM analysis.

Summary of Results

Elevated temperature compressive flow strength - strain rate properties of Ni-33Al-31Cr-3 Mo between 1200 and 1400 K have been measured for alloys directionally solidified at rates ranging from 7.6 to 508 mm/h. All the eutectics possessed statistically alike strength levels except for the alloy grown at 25.4 mm/h which was slightly stronger. While the microstructure was dependent on the growth rate, no microstructual reason could be found for this improvement. Comparison of the ~1300 K strengths of four directionally solidified NiAl-(Cr,Mo) eutectics indicates that the properties were essentially independent of Mo content between 0 to 6 at. %.

References

1. J. L. Walter and H. E. Cline, *Metall. Trans.* **1** (1970) 1221-1229.
2. H. E. Cline and J. L. Walter, *Metall. Trans.* **1** (1970) 2907-2917.
3. D.R. Johnson, X.F. Chen, B.F. Oliver, R.D. Noebe and J.D. Whittenberger, *Intermetallics* **3** (1995) 99-113.
4. T.M. Pollock and D. Kollura, Micromechanics of Advanced Materials, eds. S.N.G. Chu, P.K. Law, R.J. Arsenault, K. Sadananda, K.S. Chan, W.W. Gerberich, C.C. Chau and T.M. Kung, TMS, Warrendale, PA, 1995, pp. 205-212.
5. J. M. Yang, S. M. Jeng, K. Bain and R. A. Amato, *Acta mater.* **45** (1997) 295-305.
6. J.D. Whittenberger, S.V. Raj, I.E. Locci and J.A. Salem, *Intermetallics* **7** (1999) 1159-1168.
7. S. V. Raj, I. E. Locci and J. D. Whittenberger, Creep Behavior of Advanced Materials for the 21st Century (edited by R. S. Mishra, A. K. Mukherjee and K. Linga Murty), TMS, Warrendale, PA, 1999, pp. 295-310

8. S.V. Raj, I.E. Locci and J.D. Whittenberger, 3rd International Symposium on Structural Intermetallics (ISSI-3), eds. K.J. Hemker, D.M. Dimiduk, H. Clemens, R. Darolia, H. Inui, J.M. Larsen, V.K. Sikka, M. Thomas, J.D. Whittenberger, TMS, Warrendale, PA, 2001, pp. 785-794.
9. S. Walston and R. Darolia, 3rd International Symposium on Structural Intermetallics (ISSI-3), eds. K.J. Hemker, D.M. Dimiduk, H. Clemens, R. Darolia, H. Inui, J.M. Larsen, V.K. Sikka, M. Thomas, J.D. Whittenberger, TMS, Warrendale, PA, 2001 pp. 735-744.
10. J.D. Whittenberger, *J. Mat. Sci.* **22** (1987) 394-402.
11. K.R. Forbes, U. Glatzel, R. Darolia and W.D. Nix, *Metall. Mat. Trans.* A **27A** (1996) 1229-40.
12. J.R. Stephens and W.D. Klopp, *J. Less Com. Metals* **27** (1972) 87-94.
13. J.D. Whittenberger, Beverly Aikin, Jon Salem, *J. Mater. Res.* **16** (2001) 1333-1344.
14. S.V. Raj and I.E. Locci, *Intermetallics* **9** (2001) 217-27.
15. J.D. Whittenberger, S.V. Raj, I. Locci, and J.A. Salem, submitted to *Metal. Mat. Trans. A.*
16. D.V. Kollura and T.A. Pollock, *Acta mater.* **46** (1998) 2859-2876.
17. D. Kolluru, The creep deformation of directionally solidified NiAl-Cr and NiAl-Cr(Mo) eutectics. Ph.D. Thesis Carnegie Mellon University, Pittsburgh, PA, 1997.
18. J.D. Whittenberger, R.D. Noebe and A.Garg, *Metal. Mat. Trans. A* **27A** (1996) 3170-80.
19. O.D. Sherby, R.H. Klundt and A.K. Miller, *Metal. Trans. A* **8A** (1977) 843-50.
20. H.J. Frost and M.F. Ashby, Deformation Mechanism Maps, 1982, Pergamon Press NY, NY.
21. T.A. Venkatesh and D.C Dunand, *Metal. and Mat. Trans. A* **31A** (2000) 781-792.
22. JW Pugh, *Metal. Trans.* **4** (1973) 533-538.
23. J.L. Walter, HE. Cline, and E.F. Koch, *Trans. TMS-AIME.* **245** (1969) 2073-2079.
24. E.F. Koch, H.E. Cline, J.L. Walter, and L.M. Osika, *Acta metall.* **19** (1971) 405-414.

Figure Captions

Fig. 1. Transverse light optical, unetched microstructures of the eutectic alloys. (a) Ni-33.3Al-31.2Cr-2.9Mo directionally solidified at 7.6 mm/h, (b) Ni-33.9Al-30.8Cr-2.9Mo directionally solidified at 50.8 mm/h and (c) as-cast Ni-33.3Al-31.1Cr-3.0Mo

Fig. 2. Typical true compressive stress - strain curves for Ni-33Al-31Cr-3Mo at 1300 K as a function of the nominally imposed strain rate. (a) as-cast Ni-33.3Al-31.1Cr-3.0Mo and (b) Ni-33.0Al-32.2Cr-3.0Mo directionally solidified at 12.7 mm/h, and typical 1300 K and 1400 K compressive creep curves as a function of engineering stress for Ni-33.9Al-30.8Cr-2.9Mo directionally solidified at 50.8 mm/h. The set of open and filled symbols in (b) represent data from near duplicate test conditions.

Fig. 3. True compressive flow stress - strain rate behavior for Ni-33Al-31Cr-3Mo as a function of the directionally solidification growth rate at (a) 1200 K, (b) 1300 K and (c) 1400 K.

Fig. 4. True compressive flow stress - strain rate - temperature behavior for (a) as-cast Ni-33.3Al-31.1Cr-3.0Mo and (b) Ni-33.9Al-30.8Cr-2.9Mo directionally solidified at 50.8 mm/h. Data points from constant velocity testing are shown as open symbols, while constant load creep test results are given as solid symbols.

Fig. 5. Comparison of the true compressive flow stress - strain rate - temperature properties of Ni-33Al-31Cr-3Mo directionally solidified at 7.6, 12.7, 50.8, 127, 254, and 508 mm/h (open symbols) with those for the alloy grown at 25.4 mm/h (filed symbols).

Fig. 6. Estimated grain/cell lengths, average cell diameter, intercellular region width, interlamellar spacing, NiAl plate thickness and area fraction of the intercellular region for directional solidified Ni-33Al-31Cr-3Mo as a function of growth rate. Intercellular regions were not formed in the alloys directionally solidified at 7.6 and 12.7 mm/h and the grain diameters for these two conditions were > 1 mm.

Fig. 7. Comparison of the compressive flow stress - strain rate properties of several directionally solidified NiAl-34Cr based eutectics with/without Mo additions at/near 1300 K

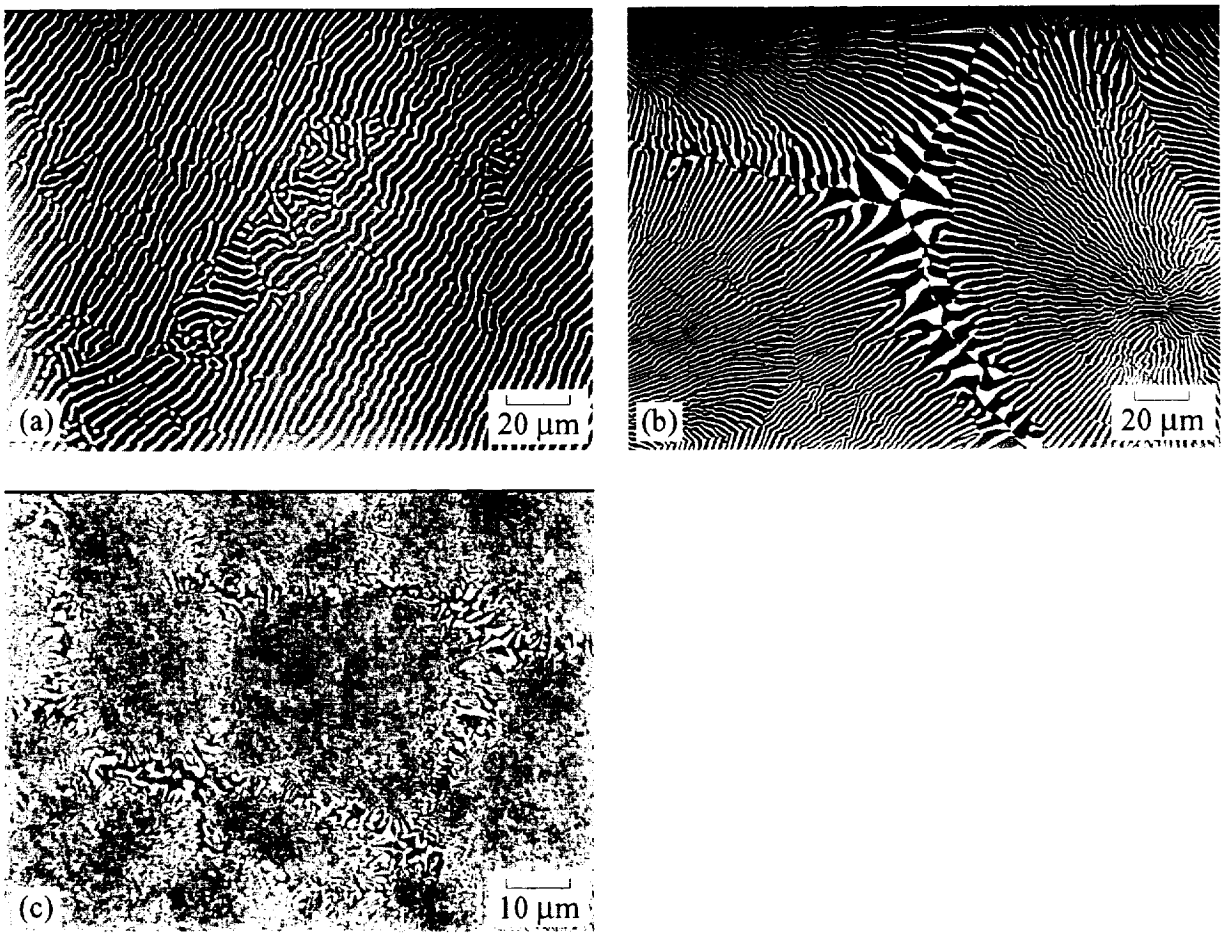

Fig 1

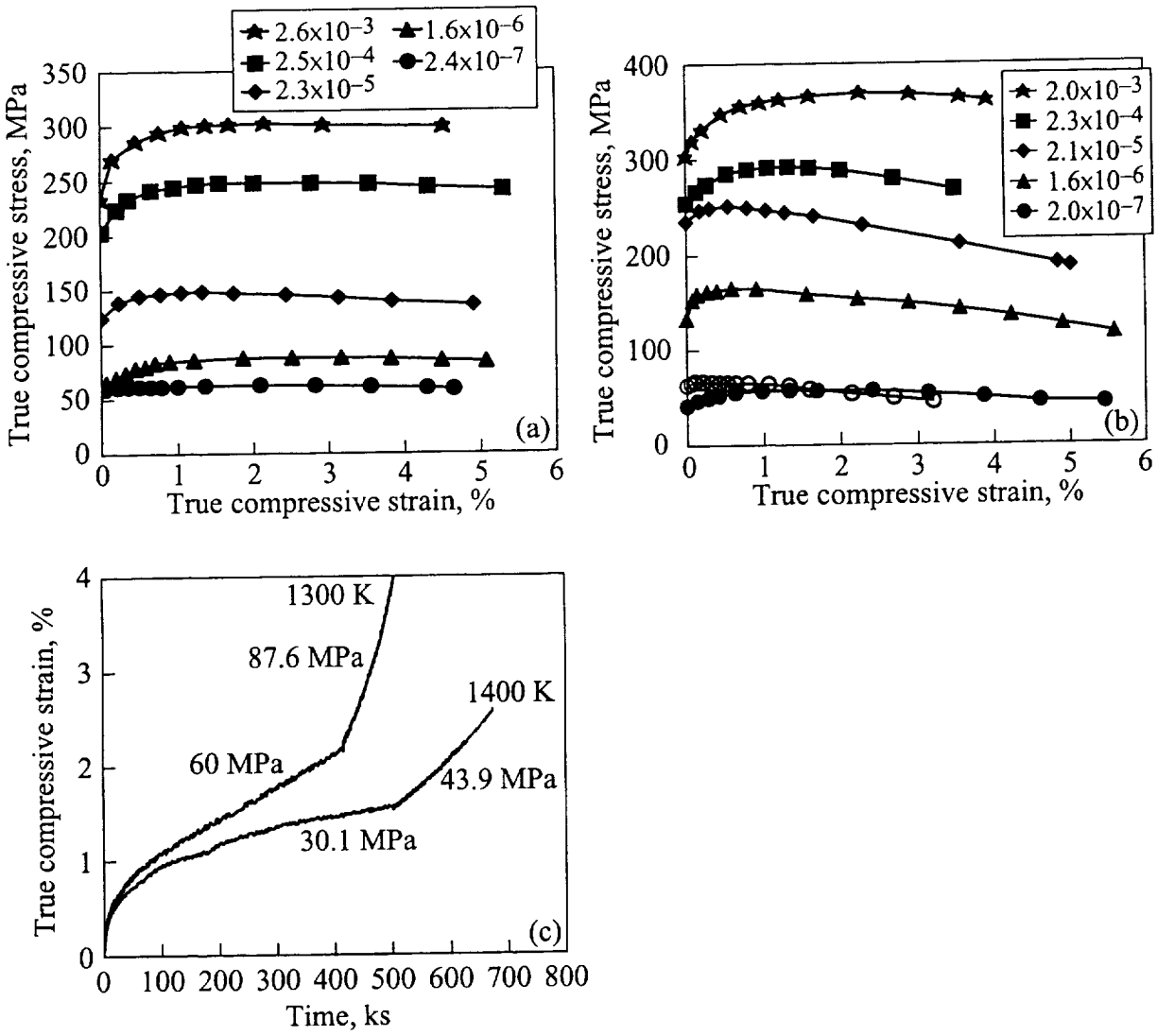
2.6x10−3
1.6x10−6
2.5x10−4
2.4x10−7
2.3x10−5
True compressive stress, MPa
True compressive strain, %
(a)
2.0x10−3
2.3x10−4
2.1x10−5
1.6x10−6
2.0x10−7
(b)
1300 K
87.6 MPa
1400 K
60 MPa
43.9 MPa
30.1 MPa
True compressive strain, %
Time, ks
(c)

Fig 2

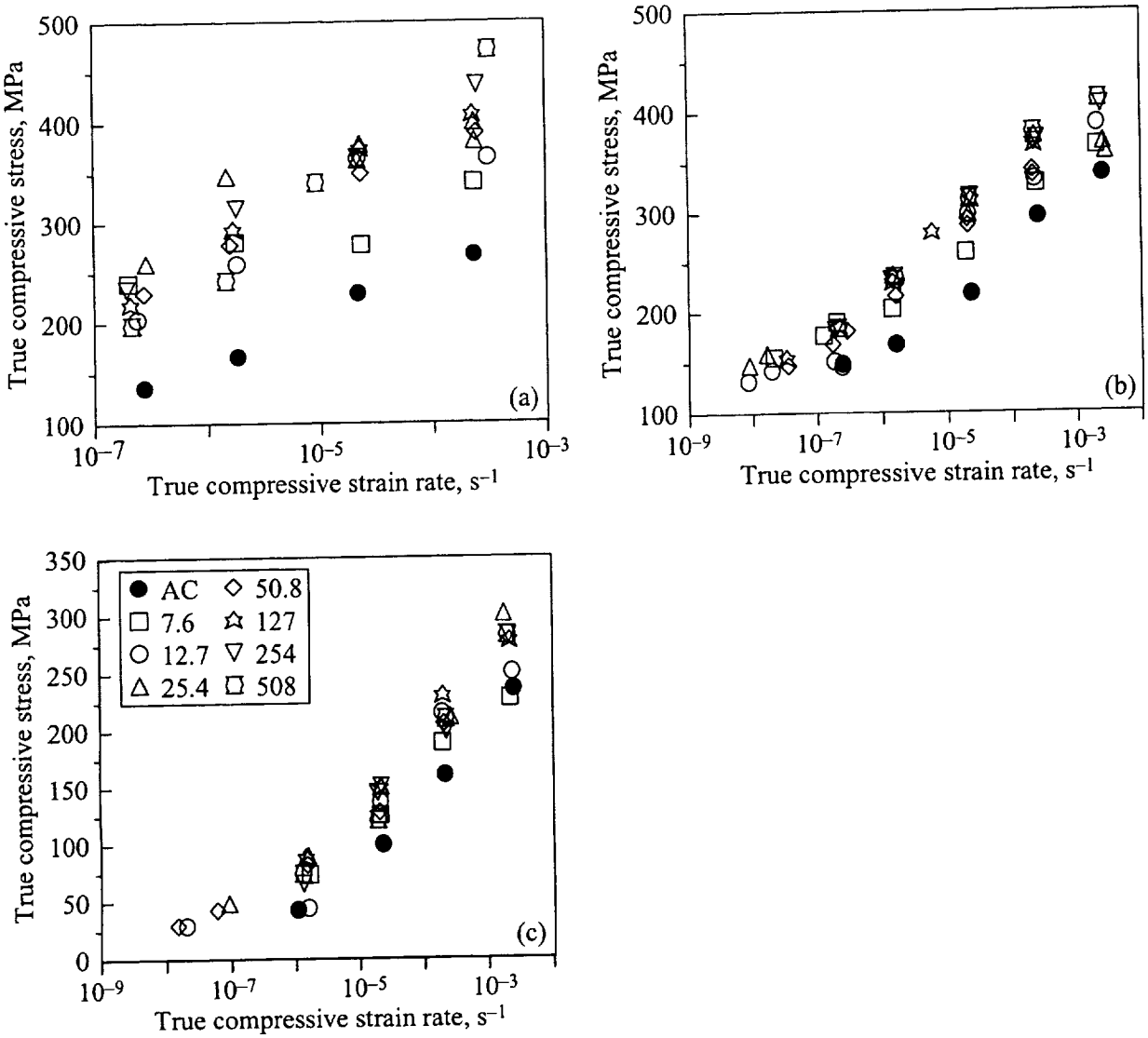
500
400
300
200
100
True compressive stress, MPa
(a)
10^{-7}
10^{-5}
10^{-3}
True compressive strain rate, s^{-1}
(b)
10^{-9}
10^{-7}
10^{-5}
10^{-3}
True compressive strain rate, s^{-1}
350
300
250
200
150
100
50
0
AC
7.6
12.7
25.4
50.8
127
254
508
(c)
10^{-9}
10^{-7}
10^{-5}
10^{-3}
True compressive strain rate, s^{-1}

Fig 3

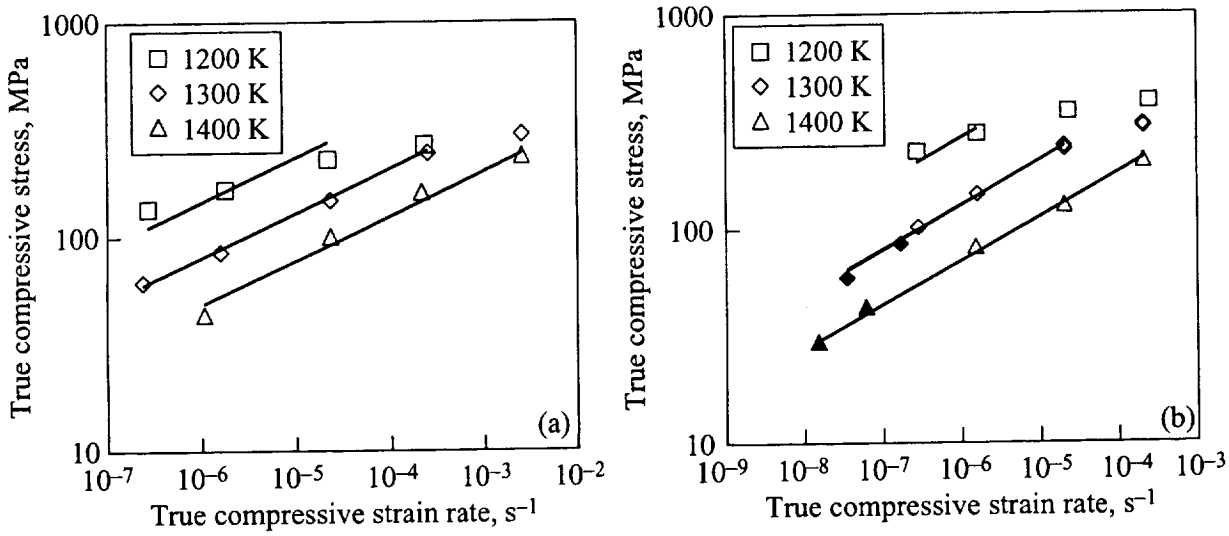
1000
100
10
True compressive stress, MPa
1200 K
1300 K
1400 K
(a)
10^{-7} 10^{-6} 10^{-5} 10^{-4} 10^{-3} 10^{-2}
True compressive strain rate, s^{-1}
1000
100
10
True compressive stress, MPa
1200 K
1300 K
1400 K
(b)
10^{-9} 10^{-8} 10^{-7} 10^{-6} 10^{-5} 10^{-4} 10^{-3}
True compressive strain rate, s^{-1}

Fig 4

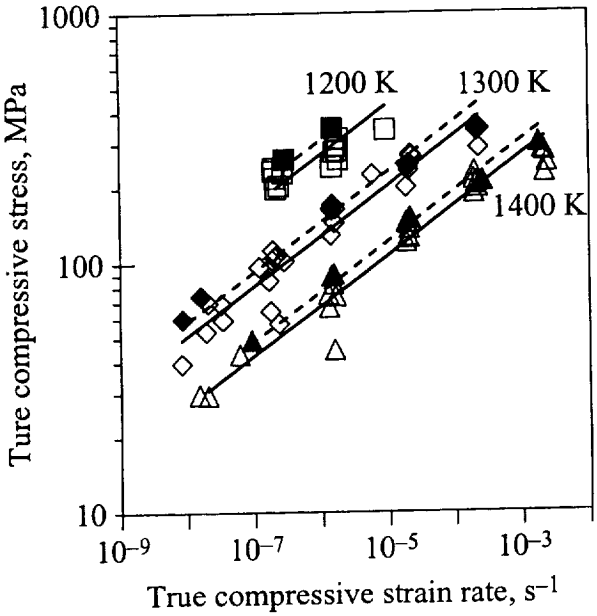
1000
100
10
1200 K
1300 K
1400 K
Ture compressive stress, MPa
10^{-9}
10^{-7}
10^{-5}
10^{-3}
True compressive strain rate, s^{-1}

Fig 5

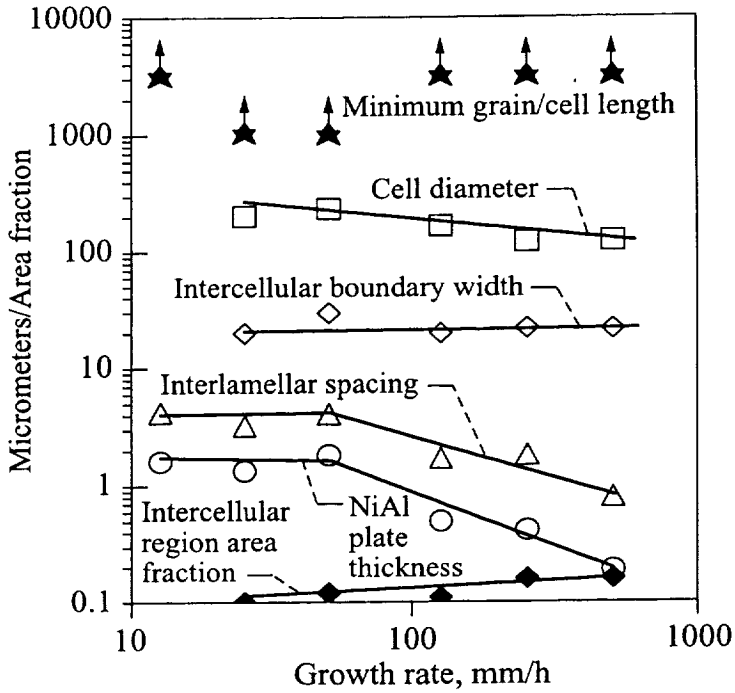
10000
1000
100
10
1
0.1
Micrometers/Area fraction
Minimum grain/cell length
Cell diameter
Intercellular boundary width
Interlamellar spacing
Intercellular region area fraction
NiAl plate thickness
10
100
1000
Growth rate, mm/h

Fig 6

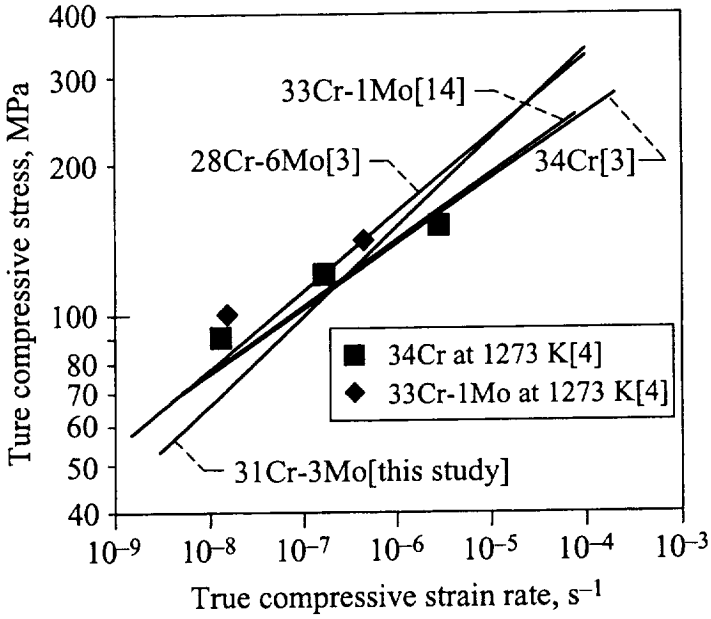
400
300
200
100
80
70
60
50
40
Ture compressive stress, MPa
33Cr-1Mo[14]
28Cr-6Mo[3]
34Cr[3]
34Cr at 1273 K[4]
33Cr-1Mo at 1273 K[4]
31Cr-3Mo[this study]
10⁻⁹
10⁻⁸
10⁻⁷
10⁻⁶
10⁻⁵
10⁻⁴
10⁻³
True compressive strain rate, s⁻¹

Fig 7